Stochastic resonance in non-dynamical systems without response thresholds

Sergey M. Bezrukov*† **& Igor Vodyanoy***‡§

* *Division of Computer Research and Technology, National Institutes of Health, Bethesda, Maryland 29892-0580, USA*
† *St Petersburg Nuclear Physics Institute, Gatchina, Russia 188530*
‡ *Office of Naval Research, Europe, 223 Old Marylebone Road, London NW1 5TH, UK*
§ *University College London, Gower Street, London, UK*

The addition of noise to a system can sometimes improve its ability to transfer information reliably. This phenomenon—known as stochastic resonance—was originally proposed to account for periodicity in the Earth's ice ages[1], but has now been shown to occur in many systems in physics and biology[2–4]. Recent experimental and theoretical work has shown that the simplest system exhibiting 'stochastic resonance' consists of nothing more than signal and noise with a threshold-triggered device (when the signal plus noise exceeds the threshold, the system responds momentarily, then relaxes to equilibrium to await the next triggering event)[4–6]. Here we introduce a class of non-dynamical and threshold-free systems that also exhibit stochastic resonance. We present and analyse a general mathematical model for such systems, in which a sequence of pulses is generated randomly with a probability (per unit time) that depends exponentially on an input. When this input is a sine-wave masked by additive noise, we observe an increase in the output signal-to-noise ratio as the level of noise increases. This result shows that stochastic resonance can occur in a broad class of thermally driven physico-chemical systems, such as semiconductor p–n junctions, mesoscopic electronic devices and voltage-dependent ion channels[7], in which reaction rates are controlled by activation barriers.

In contrast to threshold behaviour, where subthreshold forcing does not generate any output signal, threshold-free systems are able to respond to input signals of arbitrary small amplitude. We consider here threshold-free systems whose output can be described by a random train of identical pulses with the probability of pulse generation exponentially depending on the input signal. In particular, we assume that the pulse generation rate is given by:

$$r(V(t)) = r(0)\exp(V(t)) \tag{1}$$

where $r(0)$ is the 'equilibrium rate' of the pulse generation and $V(t)$ is dimensionless voltage or some other external parameter. This equation describes a broad variety of 'kT-driven' physico-chemical systems in which reaction rates are controlled by activation barriers whose heights are dependent on an external parameter. The classical examples include thermionic emission (the Richardson equation[8]), electron transfer across semiconductor p–n junctions[9], and the generalized Eyring's rate theory[10]—a foundation for kinetic phenomena description in contemporary physical and biological chemistry. Among modern examples are ion channels[7] and mesoscopic electronic devices[11].

Figure 1 illustrates the model with two examples of the output pulse train for $V(t)$ equal to zero (on the left) and for $V(t)$ randomly changing in time (on the right). It is seen that at zero input voltage the output current, $I(t)$, is represented by randomly arriving pulses. The input voltage encodes its properties into the pulse train, so that large positive deviations of the input voltage from zero substantially increase the probability of pulse generation. As a mathematical

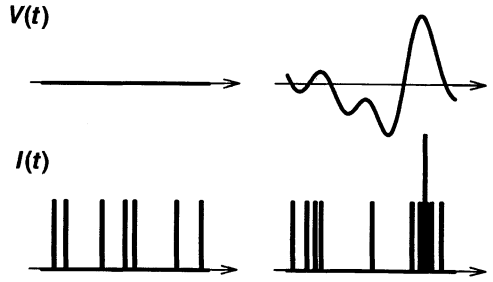

Figure 1 A time-dependent Poisson process is introduced via the voltage sensitivity of pulse generation rate. Randomly changing input voltage modulates the pulse arrival rate of an undisturbed stochastic process (tracks on the left) so that pulses start to group in time (tracks on the right). Large positive voltages increase the pulse rate to a degree where pulse overlapping is probable, and events with double (or multiple) amplitude appear in the output current.

object such a pulse train was introduced in 1955 by Cox who called it "doubly stochastic Poisson process"[12]. Following Cox, we do not discuss here the origin of initial stochasticity that leads to the pulse generation randomness—it may have different origins for different systems described by our approach, including some kind of internal fluctuation.

To facilitate subsequent treatment, we assume that $V(t)$ is the sum of a slow zero-mean gaussian noise, $V_N(t)$, and a slow small-amplitude sine-wave signal, thus limiting ourselves to the adiabatic small-signal regime:

$$V(t) = V_N(t) + V_S \sin(2\pi f_S t) \tag{2}$$

where the signal amplitude $V_S \ll 1$ and the signal frequency f_S is much smaller than all other characteristic frequencies in the model.

By analysing the statistical properties of such a pulse train we will describe the following features of signal transduction in these systems: (1) threshold-free response—the ability to transfer small signals with a transduction coefficient independent of signal amplitude; (2) noise-facilitated signal transduction—the property to increase the output signal amplitude by addition of noise to the system input; (3) noise-induced improvement in the output signal-to-noise ratio—the existence of particular input noise levels that optimize the output signal quality.

For a random train of identical pulses the statistical properties of the process are entirely defined by the moments of pulse arrival. The shape of the pulse gives only a multiplicative 'form-factor' important only at high frequencies that are comparable to inverse pulse time. To describe the signal transduction properties of our model we use the standard language of power spectral density[2–7]. At low frequencies around the signal frequency f_S, the power spectral density for this time-dependent Poisson process[13] can be written in the form:

$$S_i(f) = 2Q^2\langle r(V(t))\rangle + 4(Qr(0))^2 \times \int_0^\infty \langle \exp(V(t))\exp(V(t+\tau))\rangle \cos(2\pi f\tau)\,d\tau \tag{3}$$

where Q is single pulse area, τ is the time delay and symbol $\langle\ \rangle$ implies averaging over the ensemble representing the stochastic process. The first term here describes the frequency-independent component of noise expected from an uncorrelated time-independent train (Poisson wave) of pulses, the second one accounts for the pulse rate modulation induced by the input signal and noise (equations (1) and (2)).

For a small-amplitude signal and gaussian noise, the first term is easily expressed through the noise second moment or the root-

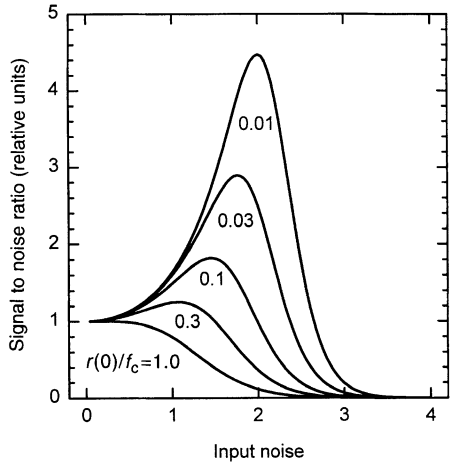

Figure 2 Output signal-to-noise ratio (SNR) can be improved by addition of the input noise. Small-signal adiabatic theory predicts the existence of optimal noise intensity corresponding to a maximum in SNR. The magnitude of the optimal input noise is sensitive to the 'equilibrium pulse rate', $r(0)$, and the noise corner frequency, f_c.

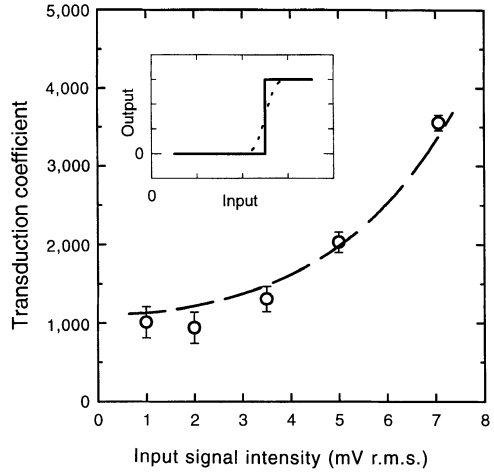

Figure 3 Signal transduction predicted by the model at zero input noise as a function of input signal intensity (dashed line) compared to those for threshold systems from electronics[16] (solid line) and biology[17] (dotted line) shown in the inset. The threshold-free character of the model is clearly seen. The points show the gain ratio measured as described in ref. 7 with the parallel array of alamethicin ion channels reconstituted in a planar lipid bilayer at 110 mV. The interrupted line is calculated for $kT/ne = 3.3$ mV.

mean-square fluctuation σ:

$$2Q^2\langle r(V(t))\rangle = 2Q^2 r(0)\exp(\sigma^2/2) \tag{4}$$

where σ, as all other voltages here, is dimensionless. To calculate the second term, we use relations for the probability density of two-dimensional normal distributions of X and Y (ref. 14) introducing the random vector (X, Y) as $X \equiv V(t)$, $Y \equiv V(t+\tau)$. After some calculations, using the condition $V_S \ll \sigma$, we obtain:

$$\langle \exp(V(t))\exp(V(t+\tau))\rangle = \exp(\sigma^2(1+\rho(\tau))) \tag{5}$$

For the band-limited 'white' noise with the corner frequency $f_c = (2\pi\tau_F)^{-1}$, the normalized autocorrelation can be written in the form:

$$\rho(\tau) = \exp(-\tau/\tau_F) + (V_S^2/2\sigma^2)\cos(2\pi f_S\tau) \tag{6}$$

At $f \ll f_c$, equation (3) becomes:

$$S_i(f) = 2Q^2 r(0)\exp\left(\frac{\sigma^2}{2}\right) + \frac{(Qr(0)\sigma)^2}{f_c}\exp(\sigma^2) \times \sum_1^\infty \frac{\sigma^{2n-2}}{n!\,n} + \frac{(Qr(0)V_S)^2}{2}\exp(\sigma^2)\delta(f-f_S) \tag{7}$$

Here, the first term on the right-hand side accounts for the noise expected from the time-independent train of pulses with the rate of $r(0)\exp(\sigma^2/2)$. The second term represents the external input voltage noise, $V_N(t)$, transduced to the output. It includes not only a small-signal part of the noise transduction but also contributions from the crosstalk between different spectral noise components. Signal transduction at $f = f_S$ is described by the term containing a delta-function. It shows that the power of the output signal grows exponentially with σ^2 and is finite at zero input noise. A d.c. component of the output is ignored.

The last two terms of equation (7) reflect the coding of the input stimulus (signal plus noise) in the pulse train. If the 'equilibrium rate' $r(0)$ were not disturbed at all, that is, if σ and V_S were zeros, these terms would vanish and would not contribute to the system output. The second term goes away also for the input noise with negligible correlations—in this case σ is held constant, but the noise corner frequency is increased to an extent where $f_c \gg r(0)\sigma^2$.

Output signal-to-noise ratio, SNR, is now easily obtained from the left part of equation (7) as the ratio of its last term to the first two:

$$\mathrm{SNR} = \frac{\frac{V_S^2 r(0)}{2\Delta f_A}\exp\left(\frac{\sigma^2}{2}\right)}{2 + \frac{r(0)}{f_c}\sigma^2\exp\left(\frac{\sigma^2}{2}\right)\sum_1^\infty \frac{\sigma^{2n-2}}{n!\,n}} \tag{8}$$

where Δf_A stands for the unit-frequency window width of the spectrum analyser that is to be used in measurements. It is seen that, except for the trivial dependence on the input signal amplitude (V_S) and the details of measurement technique (Δf_A), the SNR can be controlled by the noise intensity (σ), its frequency width (f_c), and 'equilibrium pulse rate' ($r(0)$).

Figure 2 shows the signal-to-noise ratio at different values of $r(0)/f_c$ as a function of input noise intensity. In the figure, the SNR is normalized to its magnitude at $\sigma = 0$. It can be seen that external input noise can improve the output signal quality. Noise intensity corresponding to a maximum in the output SNR increases with f_c but decreases with $r(0)$. Interestingly, however good the initial statistics (large $r(0)$), the output signal quality can be further improved if (and only if) the bandwidth of input noise is high enough for the condition $f_c > r(0)$ to hold.

It should be noted here that for small and slow signals the results of our calculations are exact. The presented model is applicable to a wide variety of systems with exponential statistics. In the case of biological ion channels the exponential statistics are due to an interaction between the part of channel molecule containing so called 'gating charges'[15] and the electric field applied across the membrane in which this molecule is embedded. For such voltage-dependent ion channels Q becomes the total charge transported through a single channel during its conductive state, and all voltages in the problem are now expressed in units of kT/ne, where ne is an effective gating charge of the channel[7].

Figure 3 shows signal transduction predicted by our model (dashed line) with experimental data obtained for voltage-dependent ion channels (data points) and demonstrates its threshold-free character. To highlight the qualitative difference, the solid and dashed lines in Fig. 3 inset describe examples of two threshold devices taken from electronics and biology: they demonstrate

the output signal of a level-crossing detector (adapted from ref. 16 for the case of zero external noise) and a nerve cell as a function of the input signal amplitude. The nerve cell is represented by the 'Hodgkin-Huxley axon' in the presence of electrical noise[17] whose magnitude determines the width of the threshold transition. It is seen that at zero external noise, the threshold devices are silent at small signals, whereas voltage-dependent ion channels transduce them with a finite coefficient. □

Received 15 July; accepted 22 November 1996.

1. Benzi, R., Sutera, S. & Vulpiani, A. *J. Phys. A* **14,** L453–457 (1981).
2. Bulsara, A. R. & Gammaitoni, L. *Phys. Today* **49,** 39–45 (1996).
3. Wiesenfeld, K. & Moss, F. *Nature* **373,** 33–36 (1995).
4. Moss, F., Pierson, D. & O'Gorman, D. *Int. J. Bifurc. Chaos* **4,** 1383–1397 (1994).
5. Wiesenfeld, K., Pierson, D., Pantazelou, E., Dames, C. & Moss, F. *Phys. Rev. Lett.* **72,** 2125–2128 (1994).
6. Gingl, Z., Kiss, L. B. & Moss, F. *Europhys. Lett.* **29,** 191–196 (1995).
7. Bezrukov, S. M. & Vodyanoy, I. *Nature* **378,** 362–364 (1995).
8. Nye, J. F. *Physical Properties of Crystals* 236–240 (Clarendon, Oxford, 1976).
9. Benedict, R. R. *Electronics for Scientists and Engineers* 80–85 (Prentice-Hall, Englewood Cliffs, 1976).
10. Glasstone, S., Laidler, K. J. & Eyring, H. *The Theory of Rate Processes* 1–27 (McGraw-Hill, London, 1941).
11. Reznikov, M., Heiblum, M., Shtrikman, H. & Mahalu, D. *Phys. Rev. Lett.* **75,** 3340–3343 (1995).
12. Cox, D. R. *J. R. Statist. Soc. B* **17,** 129–164 (1955).
13. Cox, D. R. & Lewis, P. A. W. *The Statistical Analysis of Series of Events* 28–29, 102–112 (Methuen, London, 1996).
14. Rice, S. O. in *Selected Papers on Noise and Stochastic Processes* (ed. Wax, N.) 133–294 (Dover, New York, 1954).
15. Hille, B. *Ionic Channels of Excitable Membranes* 54–47, 372–503 (Sinauer Assoc., Sunderland, 1992).
16. Jung, P. *Phys. Lett. A* **207,** 93–104 (1995).
17. Lecar, H. & Nossal, R. *Biophys. J.* **11,** 1048–1067 (1971).

Acknowledgements: We thank V. A. Parsegian for discussions and encouragement at all stages of this work; G. Weiss and M. Taqqu for consultations; V. Aguilella, B. Altshuler, C. Houdre, S. Leikin, R. Nossal, R. Podgornik and H. Strey for their suggestions and comments on the manuscripts. This work was supported by the US Office of Naval Research.

Correspondence should be addressed to S.M.B. (e-mail: bezrukov@helix.nih.gov).

Template-directed colloidal crystallization

Alfons van Blaaderen*, Rene Ruel† & Pierre Wiltzius†

* *FOM Institute for Atomic and Molecular Physics, Postbus 41883, 1009 DB Amsterdam, The Netherlands, and Van't Hoff Laboratory, Debye Institute, Utrecht University, Postbus 80051, 3508 TB Utrecht, The Netherlands*
† *Lucent Technologies, Bell Laboratories, 700 Mountain Avenue, Murray Hill, New Jersey 07974, USA*

Colloidal crystals are three-dimensional periodic structures formed from small particles suspended in solution. They have important technological uses as optical filters[1–3], switches[4] and materials with photonic band gaps[5,6], and they also provide convenient model systems for fundamental studies of crystallization and melting[7–10]. Unfortunately, applications of colloidal crystals are greatly restricted by practical difficulties encountered in synthesizing large single crystals with adjustable crystal orientation[11]. Here we show that the slow sedimentation of colloidal particles onto a patterned substrate (or template) can direct the crystallization of bulk colloidal crystals, and so permit tailoring of the lattice structure, orientation and size of the resulting crystals: we refer to this process as 'colloidal epitaxy'. We also show that, by using silica spheres synthesized with a fluorescent core[12,13], the defect structures in the colloidal crystals that result from an intentional lattice mismatch of the template can be studied by confocal microscopy[14]. We suggest that colloidal epitaxy will open new ways to design and fabricate materials based on colloidal crystals and also allow quantitative studies of heterogeneous crystallization in real space.

Epitaxial growth of a thin crystalline layer onto a template consisting of an oriented single crystal is an important process in the development of electronic devices. For instance, in molecular beam epitaxy careful control over reagent flow and temperature make it possible to achieve layer-by-layer growth of oriented crystal structures that can even be slightly out of equilibrium[15]. We have extended these ideas of template-directed crystallization to colloids, which are the ideal building blocks for photonic applications owing to their submicrometre sizes, self-organization and the possibility of chemically tailoring their properties. As a template we used a 500-nm-thick fluorescent polymer layer, with holes made with electron beam lithography (Fig. 1A). This thickness is close to the particle radius (525 nm) of the fluorescent silica spheres (fluorescent core: 200 nm). The interparticle forces are made hard-sphere-like by matching the refractive index of the solvent mixture to that of the spheres, minimizing van der Waals forces, and by increasing the ionic strength to such values that double-layer repulsion occurs over distances much smaller that the particle radius. Controlled layer-by-layer growth was achieved by slow sedimentation of the spheres onto the substrate from a volume fraction of particles well below the 50% volume fraction of homogeneous crystallization of hard-spheres[7–10]

Experimentally, hard-sphere-like colloidal dispersions are known to crystallize with a random stacking of close packed planes[7–10,16]. Theoretically, it is not clear what the thermodynamic equilibrium phase is; also, computer simulations have not been able to determine whether face-centred cubic (f.c.c., with stacking order ABC), hexagonal close packed (h.c.p., stacking ABA) or random stacking is favoured[17]. It is known, however, that thermodynamically these structures have almost the same free energy. As suggested by others[16], we found in this work that crystals that form through sedimentation have a random stacking with the close-packed planes perpendicular to gravity. Strictly speaking, a random stacked structure of close-packed planes is not a crystal, because of the randomness in one crystallographic direction. However, when a colloidal crystal was grown normal to a pattern of holes commensurate with the (100) plane of a f.c.c. crystal (Fig. 1A inset), a pure f.c.c. crystal was formed (Fig. 1B, C). By use of light scattering, we found that the f.c.c. crystal extended as far as the sedimented layer is thick (several millimetres). Also, the single crystals grew as large as the size of the pattern.

The reason for the formation of the f.c.c. crystal is that the (100) face can induce a three-dimensional structure: there is only one possible way the second layer can be placed on the holes created by the first layer. In other words, there is no twinning possibility along this growth direction (twinned crystals share a common set of atoms, but have a different orientation of their (otherwise similar) lattices). A sphere dropping into a hole 500 nm deep loses 0.6 kT in gravitational energy, where k is Boltzmann's constant and T the absolute temperature. Apparently, the small increased likelihood of a square symmetry as induced by the pattern shown in Fig. 1 is enough to start of the crystal growth with the (100) plane instead of the (111) hexagonal plane which is the densest crystal plane. For the growth of the crystal, the balance between diffusion and sedimentation is important. This balance is described by the Peclet number $\mathrm{Pe} = m_B gR/kT$, where m_B is the buoyant mass of a particle with radius R and g is the gravitational acceleration. Pe is defined as the ratio of the time it takes a particle to diffuse over a distance R and the time it takes to settle over the same distance; in this work $\mathrm{Pe} \approx 1$. For the crystal layers close to the template, the situation is very different at the end of the growth. Here the weight of several thousand layers exerts such a pressure that osmotic pressure can only balance this at a crystal volume fraction experimentally indistinguishable from close packing, 0.74.

The growth of macroscopic f.c.c. single crystals on the (110) plane, which is even less dense than the (100) plane and also has no twinning directions, was also possible. These results make it likely that the growth of pure hexagonal close-packed (h.c.p.) crystals on a non-dense h.c.p. plane that has no associated twinning direction will be feasible as well.